The effect of equivalent pressure and localized magnetism in $Cu_{1-x-y}Ag_xIr_2S_4$ system

2008 J. Phys.: Condens. Matter 20 255205

(http://iopscience.iop.org/0953-8984/20/25/255205)

J. Phys.: Condens. Matter **20** (2008) 255205 (7pp) doi:10.1088/0953-8984/20/25/255205

The effect of equivalent pressure and localized magnetism in $Cu_{1-x-y}Ag_xIr_2S_4$ system

Lei Zhang[1], Langsheng Ling[1], Shun Tan[1], Li Pi[1,2,3] and Yuheng Zhang[1]

[1] National High Magnetic Field Laboratory, University of Science and Technology of China, Hefei 230026, People's Republic of China
[2] Hefei National Laboratory for Physical Sciences at the Microscale, University of Science and Technology of China, Hefei 230026, People's Republic of China

E-mail: pili@ustc.edu.cn

Received 22 October 2007, in final form 5 April 2008
Published 19 May 2008
Online at stacks.iop.org/JPhysCM/20/255205

Abstract

The resistivity and magnetism for the $Cu_{1-x-y}Ag_xIr_2S_4$ ($x = 0$, $y = 0$, 0.05, 0.1, 0.15; $y = 0$, $x = 0$, 0.05, 0.1, 0.15) system were investigated. A Peierls-like phase transition occurs at $T_{MI} \sim 226$ K for $CuIr_2S_4$. The transition is suppressed in the $Cu_{1-x}Ag_xIr_2S_4$ system, which is attributed to that the substitution of Ag, with its larger radius, for Cu releases the pressure of Ir–Ir. The transition temperature T_{MI} increases slightly with vacancies increasing in the $Cu_{1-y}Ir_2S_4$, which corresponds to the increase of pressure. Our explanation about the pressure release and increase can also be applied to clarifying the pressure effect which is still an open question. The magnetization rises at low temperatures below T_{MI}. We suggest that it is attributed to remnant localized electrons, which do not participate in the Peierls-like phase transition, accompanied by spin-dimerization in this system. By fitting the experimental curves, we find that about 0.7% of the Ir^{4+} ions do not participate in the Peierls-like transition. The contributions of Pauli paramagnetism, Landau diamagnetism, Larmor diamagnetism and Curie magnetism can be distinguished.

(Some figures in this article are in colour only in the electronic version)

1. Introduction

Spinel compounds with the structure of AB_2X_4 (A is tetrahedral, B is octahedral) have been studied in detail in recent years because of their peculiar physical properties. For examples, $CuCo_2S_4$ exhibits antiferromagnetism with the Néel temperature $T_N = 17.5$ K and superconductivity with the transition temperature $T_S = 4.4$ K [1–4]; $CuRh_2S_4$ and $CuRh_2Se_4$ show superconductivity at $T_S = 4.7$ K and 3.5 K respectively [5]; $CuIr_2Se_4$ remains metallic down to 0.5 K and has a pressure-induced transition [6, 7]; $MgTi_2O_4$ and $CuIr_2S_4$ experience spin-Peierls-like transitions [8–10].

$CuIr_2S_4$ has a normal spinel structure with Cu^+ ions [11–13] occupying the tetrahedral sites and Ir ions occupying the octahedral sites. It undergoes a temperature-induced first-order metal–insulator transition (MIT), accompanied by the loss of localized magnetic moments at the transition temperature ($T_{MI} \sim 230$ K), called the Peierls-like transition [14, 15]. With decreasing temperature, the resistivity increases three orders of magnitude from the high temperature metallic state (HTMS) to the low temperature insulating state (LTIS), and the susceptibility drops abruptly from Pauli paramagnetism to diamagnetism due to the simultaneous spin-dimerization along ⟨110⟩ direction [10, 16–18]. In addition, $CuIr_2S_4$ also attracts attention for its many other peculiar properties [19–23], the most strange of which is that the T_{MI} increases with pressure and disappears gradually at higher pressure [24].

Although the mechanism of the Peierls-like transition in this system has been researched extensively [12, 13, 17, 25–28],

[3] Author to whom any correspondence should be addressed.

the contribution of different kinds of magnetic moments (Pauli paramagnetism, Landau diamagnetism, Larmor diamagnetism, even Curie paramagnetism) has not been clarified sufficiently yet. The rise of M in the M–T relation at low temperatures has been explained as the effect of lattice defects, called parasitic susceptibility [29]. We think that this explanation is not clear and needs to be further investigated. On the other hand, it has been reported that the pressure plays a important role in the metal–insulator transition [24]. The transition temperature T_{MI} in $CuIr_2S_4$ increases with pressure, which is the opposite to the common Mott insulator. In order to study the pressure effect, the substitution of Se, with its larger ionic radius, for S was studied [30, 31]. The transition can be suppressed by the doping of Se in $CuIr_2S_{1-x}Se_x$, but the insulator transition can be induced by pressure for $CuIr_2Se_x$ which stays metallic down to 0.5 K without applied pressure [32]. However, the doping of Se only causes average chemical pressure effects in this system.

We notice that Ag belongs to the same family as Cu, and the valence of its cation is +1. Meanwhile, the radius of the Ag ion is larger than that of Cu, so the substitution of Ag for Cu will increase the lattice of Ir–Ir, which corresponds to a release of pressure. On the other hand, vacancies in the A sites will probably reduce the distance of Ir–Ir, which corresponds to an increase of pressure. In fact, the chemical substitution and vacancies can also induce an internal pressure in the system, which makes it another efficient way to study the pressure effect on the MIT. Therefore, it is necessary to conduct a deeper study of the effect of Ir–Ir distance on the $CuIr_2S_4$ system.

2. Experiment

Polycrystalline samples of $Cu_{1-x}Ag_xIr_2S_4$ ($x = 0$, 0.05, 0.1 and 0.15) and $Cu_{1-y}Ir_2S_4$ ($y = 0.05$, 0.1, and 0.15) were prepared by the standard solid-state reaction method. The starting materials, powders of Cu (purity 99.999%), Ag (99.9%), Ir (99.95%), S (99.9999%), were mixed in the calculated ratio with 1 wt% excess S, and well ground. The mixed powder samples were sealed in vacuum quartz tubes, and heated to 1123 K at the rate of 100 K h^{-1} then held for 8 days. Then, the powder samples were reground and pressed into pellets. Finally, the pellets were sintered in vacuum quartz tubes again at 1173 K for another 2 days, then cooled down to room temperature over 10 h.

The structure and phase purity have been checked by x-ray diffraction (XRD). The XRD analysis was carried out by a Rigaku-D/max-γA diffractometer using high-intensity Cu Kα radiation at room temperature. Resistivity measurements were performed by the conventional four-probe method. The magnetic properties were measured by a superconducting quantum interference device (SQUID) MPMS system under $H = 1000$ Oe. Electron spin resonance (ESR) spectra were recorded on the powder samples in a Brucker ER200D spectrometer at 9.06 GHz.

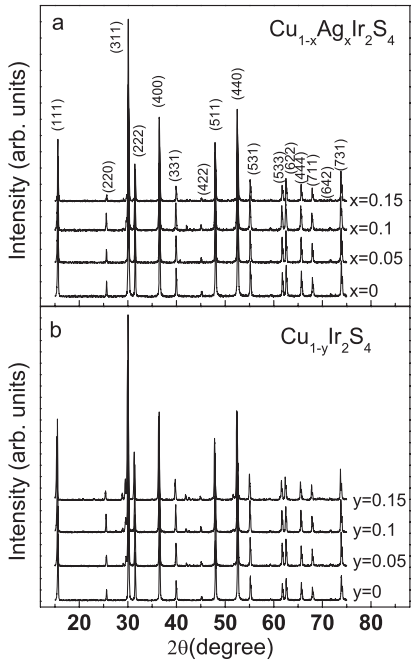

Figure 1. Powder x-ray diffraction (XRD) patterns for (a) $Cu_{1-x}Ag_xIr_2S_4$ ($x = 0$, 0.05, 0.1 and 0.15) and (b) $Cu_{1-y}Ir_2S_4$ ($y = 0$, 0.05, 0.1 and 0.15) at room temperature.

3. Results and discussion

3.1. Structural properties

XRD patterns at room temperature reveal that the structure of $Cu_{1-x}Ag_xIr_2S_4$ samples with $x \leqslant 0.15$ and $Cu_{1-y}Ir_2S_4$ with $y \leqslant 0.15$ is single phase with a spinel structure, as shown in figures 1(a) and (b). However, when x or $y \geqslant 0.2$ impurities start to appear. So our study was limited to the range of $0 \leqslant x, y \leqslant 0.15$. The crystal structure refinement was made by the Rietveld method, using the GSAS (general structure analysis system) program. The structure is cubic belonging to the space group of $Fd\bar{3}m$ at room temperature, and the lattice constant a is about 9.847 Å for $CuIr_2S_4$, consistent with another report [15]. Figure 2 shows the lattice constant a for $Cu_{1-x}Ag_xIr_2S_4$ and $Cu_{1-y}Ir_2S_4$ as function of x and y. It can be seen that the lattice constant a increases almost linearly with increasing x for $Cu_{1-x}Ag_xIr_2S_4$, which is due to the bigger radius of Ag ions, while the lattice constant a for $Cu_{1-y}Ir_2S_4$ is almost unchanged with y. The bond angle of S–Ir–S for the two system almost does not change with an increase of x or y.

3.2. Electrical resistivity

Figures 3(a) and (b) present the temperature dependence of resistivity for $Cu_{1-x}Ag_xIr_2S_4$ ($x = 0$, 0.05, 0.1, 0.15) and $Cu_{1-y}Ir_2S_4$ ($y = 0$, 0.05, 0.1, 0.15), respectively. The behaviors of resistivity for $Cu_{1-x-y}Ag_xIr_2S_4$ with different x and y are similar to each other. The resistivity is very small ($\sim 10^{-4}$ Ω cm), and decreases slightly with temperature cooling at $T \geqslant T_{MI}$. When $T \leqslant T_{MI}$, the resistivity rises suddenly about three orders of magnitude, and changes from a metallic state to an insulating state. The hysteresis

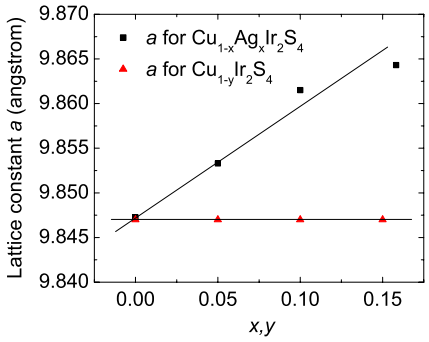

Figure 2. The x dependence of lattice constant a for $Cu_{1-x}Ag_xIr_2S_4$ (square) and the y dependence of lattice constant a for $Cu_{1-y}Ir_2S_4$ (triangle) at room temperature. The line is a guide to the eye.

upon warming and cooling at T_{MI} indicates a first-order phase transition. However, there are also some differences in resistivity for the two types of samples. The value of resistivity for $Cu_{1-x}Ag_xIr_2S_4$ at the same temperature above T_{MI} increases with x (see the inset of figure 3(a)). With an increasing content of Ag, T_{MI} moves toward lower temperatures (see inset of figure 3(a)), and the size of the jump in resistivity at T_{MI} become smaller. The value of resistivity for $Cu_{1-y}Ir_2S_4$ at the same temperature above T_{MI} also increases with y (see inset of figure 3(b)). But unlike the $Cu_{1-x}Ag_xIr_2S_4$, T_{MI} increases slightly with increasing y in $Cu_{1-y}Ir_2S_4$ (see inset of figure 3(b)). These phenomena indicate that the transition is suppressed by the doping of Ag, but strengthened by vacancies.

The replacement of Ag^+ for Cu^+ ions only changes the crystal lattice but not the electronic configuration, because the Ag^+ and Cu^+ have the same outer electronic configuration but different radii. Thus, the doping of Ag ions could not destroy the proportion of Ir^{3+} to Ir^{4+} below T_{MI}. In fact, the introduction of Ag ions causes the expansion of the lattice constant a while the bond angle of Ir–S–Ir almost stays constant. On the other hand, above T_{MI}, despite the fact that the hybridization between Ir 5d and S 3p orbits is very strong [13], the expansion of a will weaken this hybridization, consequently leading to an increase of resistivity value with increasing x in HTMS. Below T_{MI}, the Peierls-like phase transition makes the interaction of Ir–Ir occur directly through the d_{xy} orbits of Ir, which drives the electrons only hopping between the same orbits in plane (x–y plane) [17]. The elongation of Ir–Ir bonds causes the correlation between the orbits of Ir the ions to become weaker. Therefore, it can be inferred that the Peierls-like transition is suppressed. As a result, T_{MI} shifts to a lower temperature and the size of the resistivity jump is reduced at T_{MI}. The substitution of Ag for Cu has a similar effect on the lattice as the substitution of Se for S in the $CuIr_2S_4$ system. The replacement of Se for S also increases the lattice constant a [30, 31]. Compared with the doping of Ag, the vacancies in the A sites plays a different role. Generally, vacancies will cause a reduction of the distance between ions, but the lattice constant a is hardly affected by vacancies in $Cu_{1-y}Ir_2S_4$. That T_{MI} increases slightly with y in $Cu_{1-y}Ir_2S_4$ indicates that vacancies can strengthen the

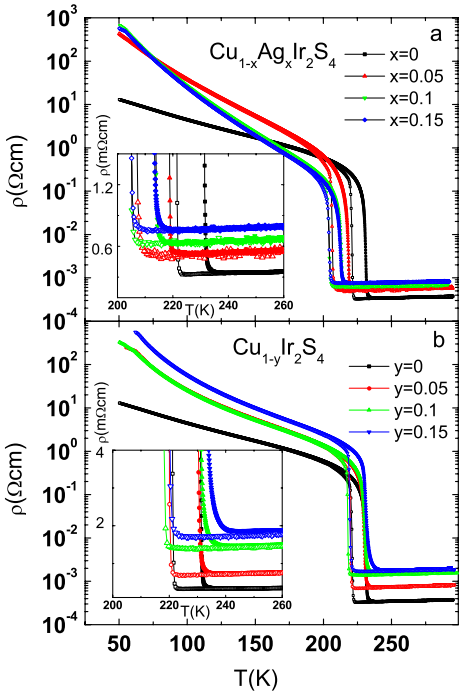

Figure 3. Temperature dependence of resistivity for (a) $Cu_{1-x}Ag_xIr_2S_4$ ($x = 0$, 0.05, 0.1 and 0.15) and (b) for $Cu_{1-y}Ir_2S_4$ ($y = 0$, 0.05, 0.1 and 0.15). The solid and open symbols are for warming and cooling, respectively. The insets are enlargements at the transition temperatures.

transition. In fact, Cu^+ ions locate in the tetrahedrons caused by S ions in the spinel structure $CuIr_2S_4$. Because the radius of the Cu^+ ion is small compared to the S ion, it lies in the holes among the S ions. The vacancies of Cu^+ hardly influence the structure, so they cannot lead to a great reduction of the distance between ions and the distance of Ir–Ir is almost unchanged. However, vacancies of Cu^+ can introduce more Ir^{4+} ions which reinforce the transition, leading to a slight increase of T_{MI}. On the other hand, the vacancies also introduce defects into this system, which leads to an increase in the potential disorder. In this case the resistivity at the same temperature above T_{MI} increases with an increase of y.

In fact, the substitution of Ag for Cu increases the bond length of Ir–S–Ir, corresponding to the release of pressure in the system, consequently weakening the hybridization between S 3p orbits and Ir 5d orbits. Therefore, T_{MI} changes to lower temperature with the release of pressure. On the contrary, the increase of the pressure leads to a shrinkage of Ir–S–Ir, which favors the Peierls-like phase transition. Thus, T_{MI} changes to a higher temperature with the increase of pressure. On the other hand, the transition can be induced by pressure for $CuIr_2Se_4$ which stays metallic down to low temperature without applied pressure [32]. That is because pressure reduces the distance of Ir–Ir in $CuIr_2Se_4$, so that the reaction can occur between the Ir ions, which are responsible for the transition.

3.3. Magnetism

The temperature dependence of magnetization for $CuIr_2S_4$ is shown in figure 4(a). With decreasing temperature,

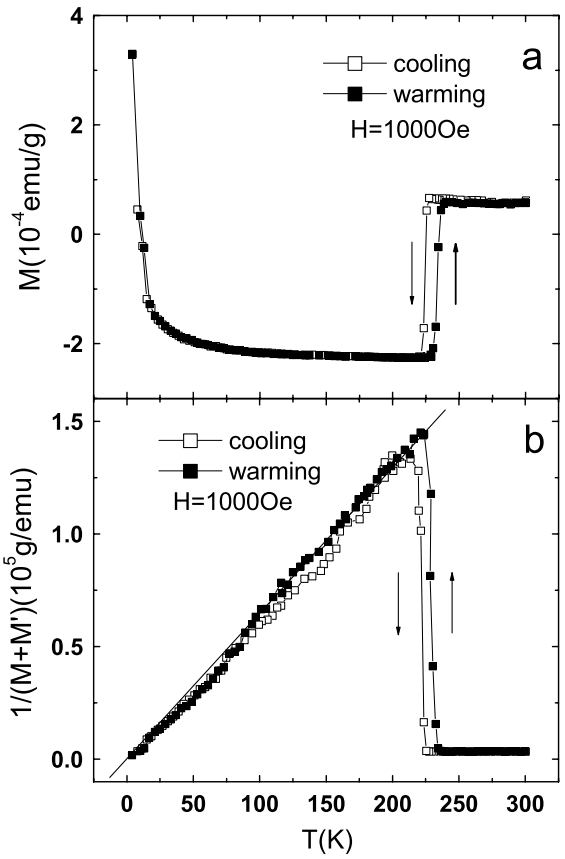

Figure 4. (a) Temperature dependence of magnetization and (b) $\frac{1}{M+M'}$–T relation for $CuIr_2S_4$ from 4 to 300 K. (M' is related to the Larmor susceptibility, and $M' \sim 2.325 \times 10^{-4}$ emu g^{-1} for $CuIr_2S_4$.) The line in (b) is a guide to the eye.

the magnetization reduces abruptly from paramagnetism to diamagnetism at T_{MI}, then stays almost independent of temperature, finally rising rapidly at low temperature to a positive value again. The hysteresis on warming and cooling at ~230 K is in agreement with the resistivity curve. The abrupt decline of magnetization at T_{MI} with cooling is due to the spin-dimerization of the Ir^{4+} ions [10].

Under ideal conditions for $CuIr_2S_4$, only free electrons contribute to the paramagnetic moments when $T > T_{\mathrm{MI}}$. So the magnetization above the T_{MI} in HTMS can be written as:

$$M_{\mathrm{HTMS}} = M_{\mathrm{Pauli}} + M_{\mathrm{Landau}} + M_{\mathrm{Larmor}}, \quad (1)$$

M_{Pauli} and M_{Landau} are Pauli paramagnetic moments and Landau diamagnetic moments respectively, both of which originate from conductive electrons. Landau diamagnetic moments cannot be detected by experiment alone because $|M_{\mathrm{Pauli}}| = 3|M_{\mathrm{Landau}}|$ in common metals, and they all disappear when conductive electrons are localized in the insulator state. M_{Larmor} are Larmor diamagnetic moments, which are produced by the Larmor motivation of electrons. After the Peierls-like phase transition, the system changes into an insulator. Radaelli *et al* suggested that antiferromagnetic dimerization occurs between Ir^{4+} and Ir^{4+} [10]. This implies that all electrons of Ir^{4+} ($S = 1/2$) form the spin-dimerization and the free electrons disappear. So both Pauli paramagnetic

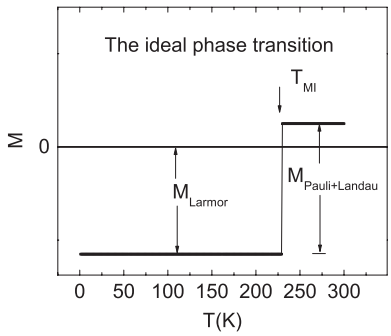

Figure 5. The M–T curve of the ideal Peierls-like phase transition.

moments and Landau diamagnetic moments disappear due to the dimerization of free electrons. The Larmor diamagnetic moments do not disappear, because they are produced by the moment $\boldsymbol{J}$ which is coupled by the orbital moment $\boldsymbol{L}$ and spin moment $\boldsymbol{S}$, and they are always negative, both above and below T_{MI}. Then the magnetization below T_{MI} in LTIS can be described as:

$$M_{\mathrm{LTIS}} = M_{\mathrm{Lamor}}. \quad (2)$$

The temperature dependence of magnetization for the ideal Peierls phase transition for $CuIr_2S_4$ is shown in figure 5.

The significant difference between the experimental curve and the ideal curve for $CuIr_2S_4$ must be emphasized. The magnetization M rises quickly at low temperature to a positive value again. This phenomenon has also been observed by others and explained as parasitic susceptibility [29, 30]. However, a further explanation has not been given yet. We notice that M is proportional to $1/T$ at low temperatures below T_{MI} if an appropriate M' is added. Figure 4(b) reveals the temperature dependence of $\frac{1}{M+M'}$ from 4 to 300 K for $CuIr_2S_4$. It can be found that the curve is a perfect line below T_{MI}. This means that the M–T relation obeys the Curie Law at low temperatures if an appropriate M' is added.

In fact, not all the electrons are free, due to the defects in the crystal. These localized electrons produce the Curie paramagnetism which is proportion to $1/T$. So experimentally, the magnetization for $CuIr_2S_4$ above the T_{MI} in HTMS could be described as:

$$M_{\mathrm{CuIr_2S_4(HTMS)}} = M_{\mathrm{Pauli}} + M_{\mathrm{Landau}} + M_{\mathrm{Larmor}} + \frac{C}{T}H, \quad (3)$$

where C is Curie constant and H is the applied magnetic field. These localized electrons do not join the Peierls-like phase transition, so the Curie magnetic moments exist at all temperatures. Thus, the magnetization below the T_{MI} in LTIS could be described as:

$$M_{\mathrm{CuIr_2S_4(LTIS)}} = M_{\mathrm{Larmor}} + \frac{C}{T}H. \quad (4)$$

Despite the fact that Curie magnetic moments are very small just below the T_{MI}, they rise with decreasing temperature. So the Larmor diamagnetic moments are gradually covered by the Curie magnetic moments with cooling.

By fitting the experimental curves (figures 4(a) and (b)), it can be found that M' relates to Larmor diamagnetic moments

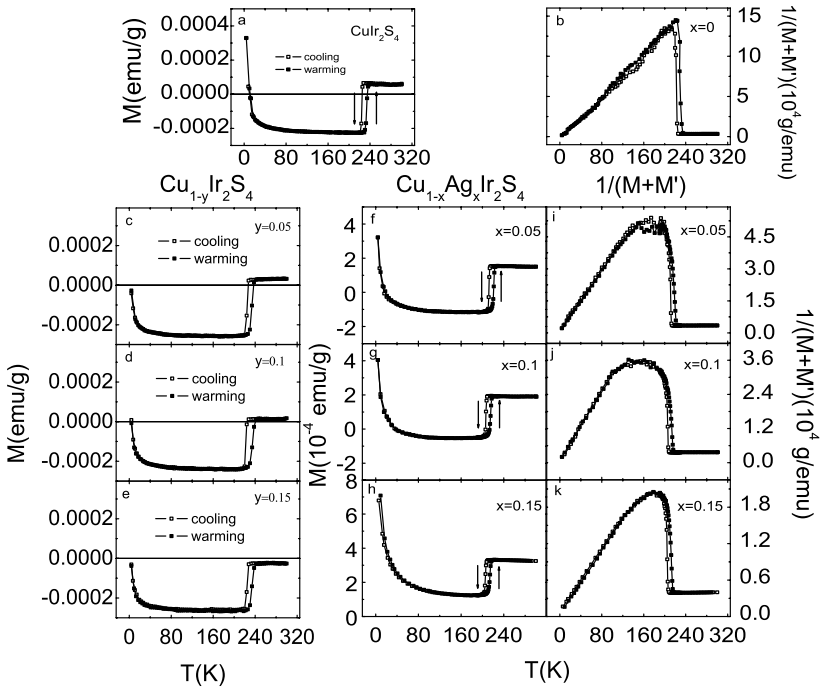

Figure 6. Temperature dependence of magnetization (measured under $H = 1000$ Oe) and inverse magnetization ($\frac{1}{M+M'}$–T relation). Figures (a) and (b) are for $CuIr_2S_4$. Figures (b)–(d) are M–T curves for $Cu_{1-y}Ir_2S_4$ ($y = 0$, 0.05, 0.1 and 0.15). Figures (e)–(j) are $\frac{1}{M+M'}$–T and M–T relations for $Cu_{1-x}Ag_xIr_2S_4$ ($x = 0$, 0.05, 0.1 and 0.15).

($M' = -M_{\text{Larmor}} = -\chi_{\text{Lamor}}H$), which are about 2.325×10^{-4} emu g^{-1}. The jump range at T_{MI} is the summation of the Pauli paramagnetic moments and Landau diamagnetic moments, ($\Delta M \approx 2.86 \times 10^{-4}$ emu g^{-1}, $H = 1000$ Oe). Finally, the calculated result shows that about 0.7% Ir^{4+} ions have Curie magnetic moments, that is to say, there are about 0.7% of the Ir^{4+} ions which have not participated in the spin-dimerization transition.

Figure 6 shows M–T and $\frac{1}{M+M'}$–T curves for $Cu_{1-y}Ir_2S_4$ and $Cu_{1-x}Ag_xIr_2S_4$. For $Cu_{1-y}Ir_2S_4$ (see figures 6(b)–(d)), the value of M above T_{MI} decreases with an increase of y, even reaching negative values for $y = 0.15$. The jump ΔM at T_{MI} also becomes smaller with increasing y. For $Cu_{1-x}Ag_xIr_2S_4$, T_{MI} shifts to lower temperatures with an increase of x. Figure 7 gives the T_{MI} judged from ρ–T and M–T curves. The jump becomes smaller with increasing x. The magnetization M rises with increasing x, and the magnetization is positive over the whole temperature range for $x = 0.15$. The same phenomenon that the $\frac{1}{M+M'}$–T relation is a perfect line below T_{MI} could also be found in the curves for the $Cu_{1-x}Ag_xIr_2S_4$ system (see figures 6(i)–(k)).

In fact, the vacancies in the A sites will cause defects in the $Cu_{1-y}Ir_2S_4$ system. As mentioned above, magnetization M above T_{MI} is mainly composed of Pauli paramagnetism, Landau diamagnetism and Larmor diamagnetism. Pauli paramagnetism and Landau diamagnetism are produced by free electrons, and Larmor diamagnetism originates from the Larmor motivation of $\boldsymbol{J}$. The defects caused by the vacancies in the A sites will block the motivation of free electrons, resulting in the reduction of both Pauli paramagnetism and Landau diamagnetism. Consequently, the summation of Pauli

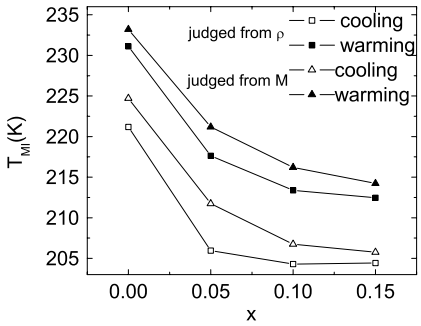

Figure 7. The transition temperature (T_{MI}) as function of the doping density x for $Cu_{1-x}Ag_xIr_2S_4$ ($x = 0$, 0.05, 0.1 and 0.15), judged from resistivity and magnetization curves, respectively.

paramagnetism and Landau diamagnetism, which is positive above T_{MI}, decreases with the increase of y. Then both the magnetization M above T_{MI} and the jump range ΔM decrease with increasing y. The value of Larmor diamagnetism above T_{MI} gradually overcomes the sum of the Pauli paramagnetism and Landau diamagnetism with increasing y, finally leading to the appearance of diamagnetism above T_{MI} for $y = 0.15$. For $Cu_{1-x}Ag_xIr_2S_4$, the substitution of Ag for Cu can suppress the Peierls-like transition because of the extension of Ir–Ir. That the jump range of M at T_{MI} becomes smaller implies that the Pauli paramagnetic moments becomes smaller. The value of M rises with increasing x, and even M below T_{MI} becomes positive for all temperatures for $x = 0.15$. This is because the doping of Ag ions causes localized electrons which produce Curie paramagnetic moments. The value of M is raised by this Curie paramagnetism.

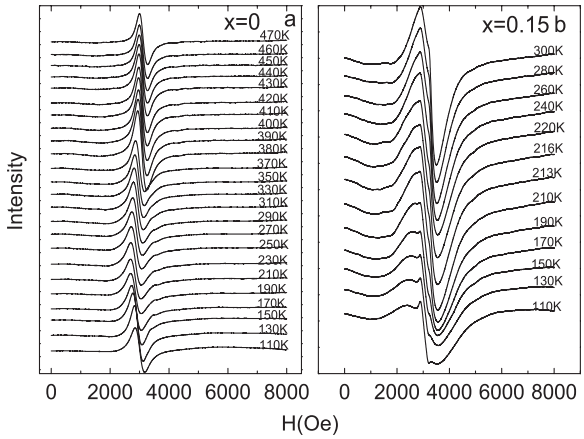

Figure 8. ESR spectra for $Cu_{1-x}Ag_xIr_2S_4$ samples ($x = 0$ and 0.15) at different temperatures.

In order to verify the existence of Curie paramagnetic ions, we took measurements of electron spin resonance (ESR) spectra. The ESR spectra for $Cu_{1-x}Ag_xIr_2S_4$ ($x = 0$ and 0.15) at different temperatures are shown in figure 8. Similar signals are detected in all the samples. The ESR signals with $g \approx 2$ are always found, both above and below T_{MI}, and have experience no abrupt change at T_{MI}. This indicates that the paramagnetism is always present and does not change at T_{MI}. That is to say, the paramagnetism has nothing to do with the Peierls-like transition. In fact, the paramagnetic ESR signals originate from the localized electrons which have not joined in the transition.

4. Conclusion

The Peierls-like phase transition material $Cu_{1-x-y}Ag_xIr_2S_4$ ($x = 0$, $y = 0$, 0.05, 0.1, 0.15; $y = 0$, $x = 0$, 0.05, 0.1, 0.15) system was studied. In the $Cu_{1-x}Ag_xIr_2S_4$ system, the T_{MI} moves to lower temperatures and the jump range at T_{MI} becomes smaller with increasing x. However, T_{MI} remains unchanged in the $Cu_{1-y}Ir_2S_4$ system, and the jump range ΔM in magnetization becomes smaller with increasing y. Diamagnetism even appears above T_{MI} for $Cu_{1-y}Ir_2S_4$ with $y = 0.15$. This indicates that the substitution of Ag^+ for Cu^+ suppresses the Peierls-like phase transition, but the vacancy in A site has little effect on the Peierls-like phase transition. However, the vacancies can reduce both the Pauli paramagnetism and Landau diamagnetism. This can be explained through the lattice effects. The explanation could also be applied to clarify the pressure effect. From the rapid rise of M at low temperature below T_{MI} in M–T curve, we notice that M is proportional to $1/T$ at low temperature below T_{MI} if an appropriate M' is added. There are remnant localized electrons which do not participate in the Peierls-like phase transition accompanied by the spin-dimerization in this system. By fitting the $\frac{1}{M+M'}$–T curve, it can be found that only about 0.7% of the Ir^{4+} ions have not participated in the Peierls-like transition, and the localized electrons of this fraction contribute to the Curie magnetization. The Pauli paramagnetism disappears when the transition occurs. In this case the fitting parameter M' just relates to the Larmor diamagnetism ($M' = |M_{Larmor}| = -\chi_{Larmor}H$). By fitting to the experimental curves, we can distinguish the contributions of Pauli paramagnetism, Landau diamagnetism, Larmor diamagnetism and Curie magnetism. The ESR spectra confirm the existence of Curie paramagnetism.

Acknowledgments

The authors would like to thank Professor Yuping Sun (Institute of Solid State Physics, Chinese Academy of Sciences) for the sample preparation. This work was supported by the National Nature Science Foundation of China (Nos 10334090 and 10504029), and the State Key Project of Fundamental Research of China (2007CB925001).

References

[1] Nishihara N, Kanomata T, Kaneko T and Yasuoka H 1991 *J. Appl. Phys.* **69** 4618
[2] Sugita H, Wada S, Miyatani K and Tanaka T 1998 *J. Phys. Soc. Japan* **67** 1401
[3] Nishikawa T, Ueda H, Tanaka T and Miyatani K 2000 *Proc. Int. Conf. on Ferrites (Kyoto)* p 241
[4] Sugita H, Wada S, Miyatani K, Tanaka T and Ishikawa M 2000 *Physica* B **284–288** 473–4
[5] Hagino T, Seki Y, Wada N, Tsuji S, Shirane T, Kumagai K I and Nagata S 1995 *Phys. Rev.* B **51** 12673
[6] Tang J, Matsumoto T, Furubayshi T, Kosaka T, Nagata S and Kato Y 1998 *J. Magn. Magn. Mater.* **177–181** 1363–4
[7] Burkov A T, Nakama T, Hedo M, Shintani K, Yagassaki K, Matsumoto N and Nagata S 2000 *Phys. Rev.* B **61** 10049
[8] Schmidt M *et al* 2004 *Phys. Rev. Lett.* **92** 056402
[9] Zhou H D and Goodenough J B 2005 *Phys. Rev.* B **72** 045118
[10] Radaelli P G, Horibe Y, Gutmann M J, Ishibashi H, Chen C H, Ibberson R M, Koyama Y, Hor Y-S, Kiryukhin V and Cheong S-W 2002 *Nature* **416** 155
[11] Matsuno J, Mizokawa T, Fujimori A, Zatsepin D A, Galakhov V R, Kurmaev E Z, Kato Y and Nagata S 1997 *Phys. Rev.* B **55** R15979
[12] Kumagai K, Tsuji S, Hagino T and Nagata S 1995 *Spectroscopy of Mott Insulators and Correlated Metals* ed A Fujimori and Y Tokura (Berlin: Springer) p 255
[13] Oda T, Shirai M, Suzuki N and Motizuki K 1995 *J. Phys.: Condens. Matter* **7** 4433
[14] Nagata S, Hagino T, Seki Y and Bitoh T 1994 *Physica* B **194–196** 1077–8
[15] Furubayashi T, Matsumoto T, Hagino T and Nagata S 1994 *J. Phys. Soc. Japan* **63** 3333
[16] Kang H, Mandal P, Medvedeva I V, Liebe J, Rao G H, Barner K, Poddar A and Gmelin E 1998 *J. Appl. Phys.* **83** 1
[17] Khomskii D I and Mizokawa T 2005 *Phys. Rev. Lett.* **94** 156402
[18] Yagasaki K, Nakama T, Hedo M, Uwatoko Y, Shimoji Y, Notsu S, Yoshida H, Kimura H M, Yamaguchi Y and Burkov A T 2006 *J. Phys. Soc. Japan* **75** 074706
[19] Suzuki H, Furubayashi T, Cao G, Kitazawa H, Kamimura A, Hirata K and Matsumoto T 1999 *J. Phys. Soc. Japan* **68** 2495
[20] Cao G, Furubayashi T, Suzuki H, Kitazawa H, Matsumoto T and Uwatoko Y 2001 *Phys. Rev.* B **64** 214514
[21] Cao G, Naka T, Kitazawa H, Isobe M and Matsumoto T 2003 *Phys. Lett.* A **307** 166
[22] Ishibashi H, Koo T Y, Hor Y S, Borissov A, Radaelli P G, Horibe Y, Cheong S-W and Kiryukhin V 2002 *Phys. Rev.* B **66** 144424

[23] Sun W, Kimoto T, Furubayashi T, Matsumoto T, Ikeda S and Nagata S 2001 *J. Phys. Soc. Japan* **70** 2817
[24] Oomi G, Kagayama T, Yoshida I, Hagina T and Nagata S 1995 *J. Magn. Magn. Mater.* **140–144** 157–8
[25] Kitamoto K, Taguchi Y, Mimura K, Ichikawa K, Aita O and Ishibashi H 2003 *Phys. Rev.* B **68** 195124
[26] Chitov G Y and Gros C 2004 *Phys. Rev.* B **69** 104423
[27] Kurmaev E Z, Galakhov V R, Zatsepin D A, Trofimova V A, Stadler S, Ederer D L, Moewes A, Grush M M, Gallcott T A, Matsuno J, Fujimori A and Nagata S 1998 *Solid State Commun.* **108** 235
[28] Croft M, Caliebe W, Woo H, Sills D, Hor Y S, Cheongv S W, Kiryukhin V and Oh S J 2003 *Phys. Rev.* B **67** 201102
[29] Kang H, Barner K, Rager H, Sondermann U, Mandal P, Medvedeva I V and Gmelin E 2000 *J. Alloys Compounds* **306** 6–10
[30] Nagata S, Matsumoto N, Kato Y, Furubayashi T, Matsumoto T, Sanchez J P and Vulliet P 1998 *Phys. Rev.* B **58** 6844
[31] Somasundaram P *et al* 1998 *J. Appl. Phys.* **83** 7243
[32] Furubayashi T, Kosaka T, Tang J, Matsumoto T, Kato Y and Nagata S 1997 *J. Phys. Soc. Japan* **66** 1563